

Airborne Infrared Scanning Imaging System with Rotating Drum for Fire Detection

Dalin Song¹, Jun Chang^{1*}, Jiao Cao¹, Lifei Zhang¹, Yao Wen¹, Aman Wei¹, and Jiang Li²

¹*School of Optoelectronic, Beijing Institute of Technology, Beijing 100081, China*

²*Patent Examination Cooperation Center of SIPO, Beijing 100190, China*

(Received October 17, 2011 : revised November 21, 2011 : accepted November 23, 2011)

Airborne infrared techniques have been used in wild land fire management for decades. This paper describes a kind of infrared scanning system based on a rotating drum with a tilted porthole underside the plane nose. This design increases the stability of the mechanism system, reduces air resistance and protects inner parts. Aberration characteristics of a tilted ellipsoid porthole are analyzed and an effective solution is invented which makes the system achieve 30° field of regard. The system's ultimate value of modulation transfer function is near the diffraction limit, which indicates that the performance of the rotating optical system meets the imaging requirements.

Keywords : Lens system design, Geometric optical design, Rotating drum scanning, Tilted porthole, Aberration correction

OCIS codes : (080.3620) Lens system design; (220.2740) Geometric optical design

I. INTRODUCTION

The controlled use of fire is an impetus to human civilization, but the runaway forest fire can cause great damage and the loss of life and property. The airborne infrared (IR) detection technique has been applied in the area of wild land fire detection for nearly half a century. It is widely used to detect, monitor, and orientate fire suppression and mop-up operations. Tradition infrared systems are mounted in two styles --nadir or gimbale. The sensor is pointed directly below the plane belly and provides a relatively narrow field of view with nadir mounts. These systems are capable of imaging a large incident promptly, and help the fire managers to get a snapshot of the conditions. With gimbale mounts, widely known as forward-looking IR (FLIR) balls, the IR equipment mounted on a stabilized turret pointing nearly any direction is not masked by the plane body, and is very practical for fire-line mapping and mop-up operations. They scan the object from different angles, thus the FLIR can discover fire which may elude nadir-mounted systems. However few of FLIR balls are mounted on fixed winged aircraft as most civilian planes have a low body and the turret is protruding beneath the plane chassis. Stones rising from airfield runway are likely to crush the FLIR window as

the plane taxis. Besides, the projecting turret increases air resistance and reduces cruising speed.[1-4]

According to the above analysis it is necessary to investigate an improved airborne IR detection system which is inside the plane body to avoid injury, mounts with a tilted porthole conformal to the prow for decreasing air drag and has an appropriate scanning mechanism able to provide a large field of view.

II. ABERRATION ANALYSIS AND CORRECTION

2.1. Tilted Glass Porthole Aberration Analysis

The nose of a firefighting cruising plane model could be simplified as an ellipsoid. A typical value of the ellipsoid length divided by the height can be taken as 2.

Fig. 1 shows the layout of the ellipsoidal plane nose with a perfect lens at four different scanning positions from -30° to -60° in 10° increments. Fig. 2 shows large amplitude selected Zernike aberrations across the wide FOR (Field of regard -the area covered for the detector of the system when pointing to all possible mechanically positions⁵). As shown in the chart (wavelength = 4 μm) the dominant aberrations caused by an ellipsoidal dome are 3rd order

*Corresponding author: bitchang@bit.edu.cn

Color versions of one or more of the figures in this paper are available online.

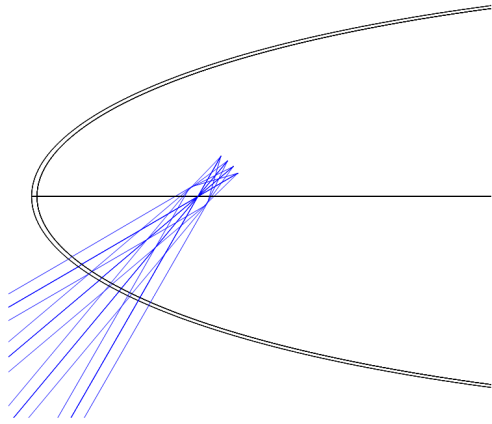


FIG. 1. Layout of ellipsoidal nose porthole with a perfect lens.

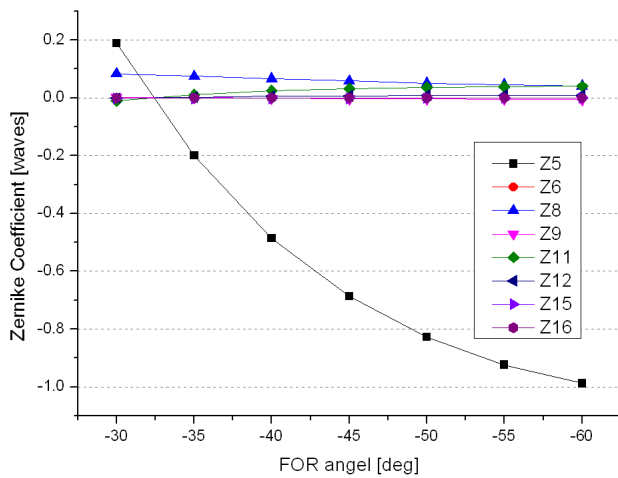


FIG. 2. Selected Zernike aberrations.

astigmatism (Z5). So the fundamental challenge is to find an appropriate scheme to correct this large aberration.

2.2. Theory of Primary Aberration for the Ellipsoidal Surface

Aberration characteristics of the ellipsoidal surface are similar to those of a spherical surface except for the distribution among surfaces. To calculate the primary aberration distribution of an ordinary aspheric surface, one ellipsoidal surface can be considered as the overlap of one spherical surface and another zero center thickness plate as shown in Fig. 3, where the z axis is the optic axis, r axis is the meridian plane coordinate axis, O is the origin of coordinates, r_0 is the datum surface radius, c is the center of curvature, Δz is thickness increment of the zero center thickness plate, n and n' are material refractive indices before and after the surface respectively.

Relative to a spherical surface which has the same axial curvature radius r_0 , the 3rd order astigmatism aberration coefficients increment of the ellipsoidal surface can be

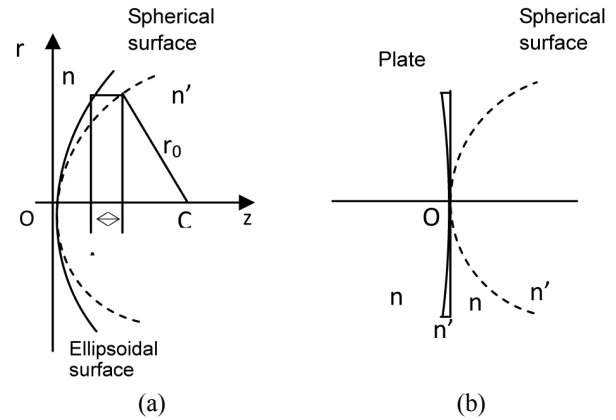


FIG. 3. Overlap of zero center thickness plate and one spherical surface.

described as

$$\Delta S_3 = -\frac{(n'-n)e^2}{r_0^3} h^2 \cdot h_z^2 \quad (1)$$

where h is the intersection height of the paraxial ray on the aspheric plate, h_z is the intersection height of the chief ray on the aspheric plate, and e is eccentricity.[6-8]

The additional aberrations induced by the ellipsoid surface ($0 < e^2 < 1$) could be described by the above expression (1). Because the e^2 increment is in direct proportion to $-e^2$, an oblate element ($e^2 < 0$) can provide balance of additive 3rd order astigmatism induced by the ellipsoidal porthole ($0 < e^2 < 1$). The opposite signed additive aberrations can be cancelled out for different conic surfaces. We suppose that one conic plate corrector could correct the additional aberrations induced by an ellipsoid optical window with appropriate aperture position.

2.3. Oblate Corrector for Ellipsoid Nose Porthole

The ellipsoid MgF_2 porthole glass is to be compensated in this design. We take advantage of the powerful features of commercially-available optical design software to optimize the oblate correction element. Fig. 4 shows the system layout followed by a perfect F/4 lens at 4200 nm wavelength across the -30° to -60° FOR. Zernike aberrations are analyzed with and without the oblate corrector respectively as shown in Fig. 5 (wavelength = 4 μm), which indicates that the corrector has compensated the 3rd order stigmatism to a great extent.

III. SCANNING OPTICAL SYSTEM DESIGN

3.1. System Scheme and Specifications

Fig. 6 shows the design of a complete scanning IR optical system with tilted MgF_2 porthole, oblate corrector, rotating drum and imaging lens. The porthole glass and

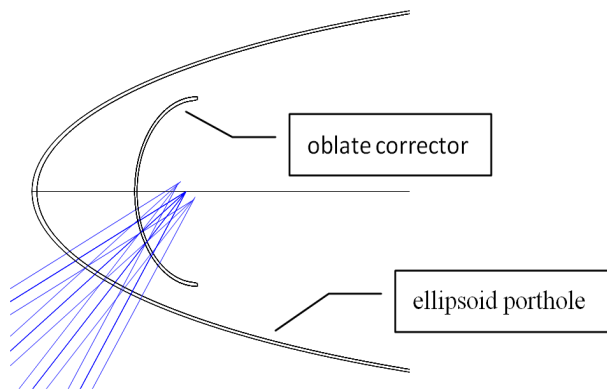


FIG. 4. Ellipsoid MgF_2 porthole glass with one oblate corrector.

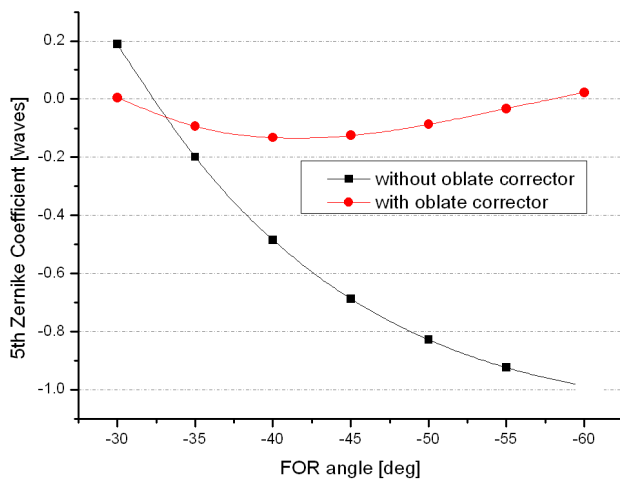


FIG. 5. The 5th Zernike aberrations with and without corrector.

TABLE 1. Relevant specifications for the entire IR optical system

Spectral band	3800nm to 4600nm
F/#	4.0
Focal length	172mm
FOR	-30° to -60°
IFOV	$\pm 2^\circ$

oblate corrector are similar to those analyzed in section 2.3. Table 1 lists the design specifications. IFOV means the instantaneous field of view.

3.2. Simulations and Optimizations Methodology

The complete system layout shown in Figure 6 is the result of a stepwise design process. A reflective rotating drum is adopted for scanning the target fire. The drum center is located on the optical axes of the MgF_2 porthole and the oblate corrector. The subsequent imaging system is a conventional secondary imaging structure. It has 100%

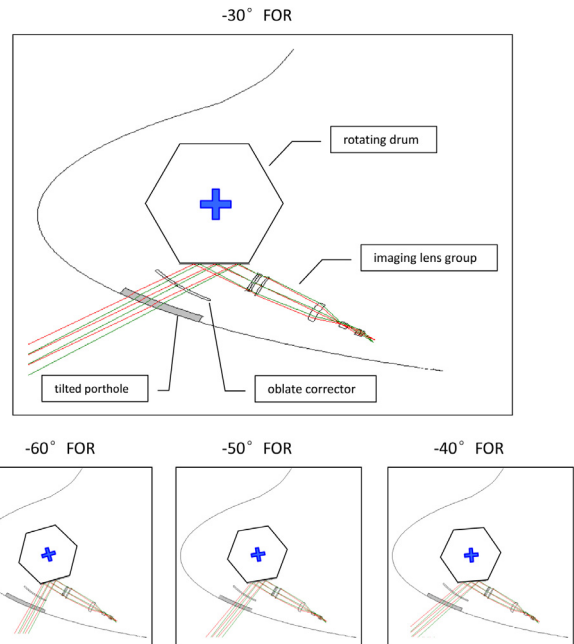


FIG. 6. IR scanning system with tilted MgF_2 porthole, oblate corrector, oscillating mirror and imaging lens group.

TABLE 2. Imaging lens surface parameters

Lens	Surface radius (mm)	Thickness (mm)	Glass
Lens 1	194.73	3.47	Silicon
	271.11	0.17	
Lens 2	372.01	3.39	Germanium
	118.94	10.18	
Lens 3	198.74	4.01	Silicon
	-1049.49	102.32	
Lens 4	63.59	12.39	Silicon
	90.06	44.67	
Lens 5	-14.46	14.23	Silicon
	-21.22	18.28	
Lens 6	164.25	2.74	Germanium
	-428.70	3.38	
Lens 7	16.18	5.49	Silicon
	17.20		

cold shield efficiency and can reduce the radial size of the system.[9] Ultimate optimization of the complete structure for all four different FOR position results in the final design. Table 2 lists detailed imaging lens surface parameters.

3.3. Results

The system's ultimate modulation transfer function (MTF) of the IR scanning optical system is approximately at the diffraction limit as shown in Fig. 7.

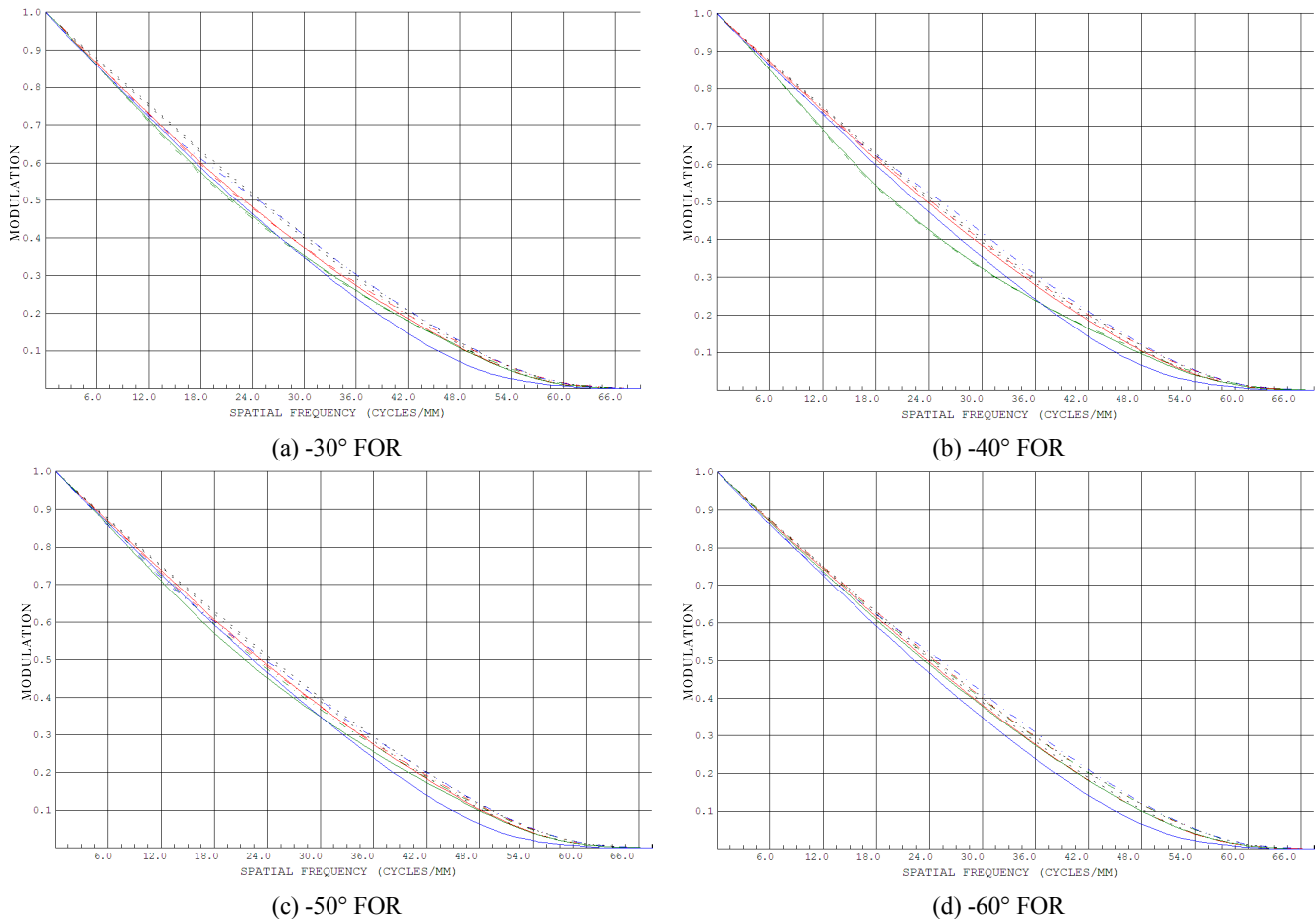


FIG. 7. System's ultimate value of modulation transfer functions.

TABLE 3. Some tolerance items of the corrector

Thickness Delta (mm)	0.1
Total Wedge (mm)	0.1
Barrel Tilt (radians)	0.01
Element Decenter (mm)	0.1
Random RMS Surface Error (waves)	1.0

TABLE 4. Probable change in MTF for 20 cycles/mm

Change in MTF FOR	IFOV		
	0°	2.8°	4°
-30°	-0.0284	-0.0363	-0.0307
-40°	-0.0196	-0.0182	-0.0198
-50°	-0.0182	-0.0248	-0.0218
-60°	-0.0143	-0.0157	-0.0154

Table 3 lists some of tolerance items of the corrector and Table 4 lists the probable change in MTF for 20 cycles/mm at 97.7% cumulative probability.

IV. CONCLUSIONS

We have shown the design of an IR scanning optical system for airborne wild land fire detection equipment with a rotating drum. The reflective drum is an effective and practical way to scan large FOR and also the oblate corrector is appropriate in compensating aberrations arising in a tilted porthole. This optical system provides an easy-fabrication and low-cost scheme for land wildfire alarms.

REFERENCES

1. J. Johnson, Remote Sensing Applications Center, Phoenix and Infrared Imagery Interpretation: Changes to Wild Land Fire Incident Support Over the Past Five Years RS2008.
2. United States Department of Agriculture Forest Service-Engineering, Remote Sensing Applications Center, Infrared Field Users' Guide and Vendor Listings, October 2003 RSAC-1309-RPT1.
3. Y. Chung, B. Lee, and S. Kim, "Optimal shape design of dielectric micro lens using FDTD and topology optimization," *J. Opt. Soc. Korea* **13**, 286-293 (2009).
4. C. Rim, "The optical design of miniaturized microscope

- objective for CARS imaging catheter with fiber bundle,” J. Opt. Soc. Korea **14**, 424-430 (2010).
5. <http://en.allexperts.com/q/Satellite-Communications-2436/f/Field-Regard-Field-View.htm>.
 6. Y. M. Zhang, “Primary aberration of aspheric surface,” in *Applied Optics* (Publishing House of Electronics Industry, Beijing, China, 2008).
 7. W. J. Smith, “Third-order aberrations- contributions from aspheric surface,” in *Modern Lens Design* (McGraw-Hill Companies, New York, USA, 2005).
 8. D. L. Song, J. Chang, Q. F. Wang, W. B. He, and J. Cao, “Conformal optical system design with a single fixed conic corrector,” J. Chin. Phys. B **20**, 0742-01 (2011).